Patient-specific in-vivo QA in MRGRT: 3D EPID dosimetry for the Unity MR-linac

Torres Xirau, I.

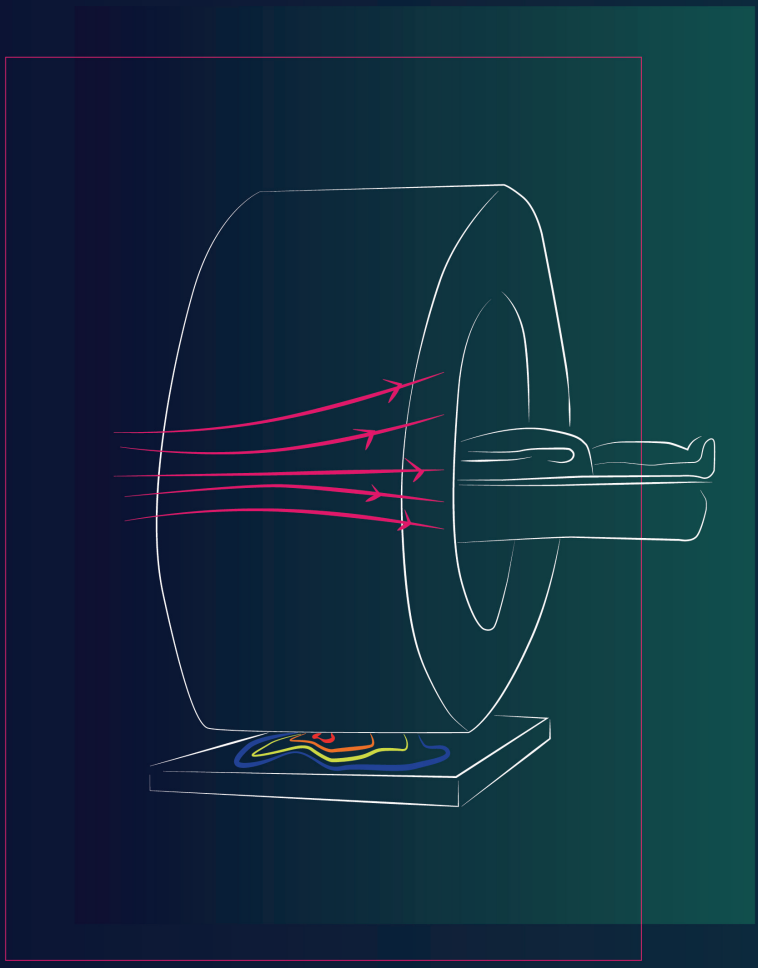

5.

3D DOSIMETRIC VERIFICATION OF UNITY MR-LINAC TREATMENTS BY PORTAL DOSIMETRY.

Iban Torres-Xirau
Igor Olaciregui-Ruiz
Jochem Kaas
Marlies E. Nowee
Uulke A. van der Heide
Anton Mans

Department of Radiation Oncology,
The Netherlands Cancer Institute–Antoni van Leeuwenhoek Hospital,
Plesmanlaan 121, 1066 CX Amsterdam, The Netherlands

Radiotherapy and Oncology, Volume 146, Number 9, Pages 161-166
Published March 2020•

Abstract

3D dosimetric verification of online adaptive workflows is essential as their complexity is unprecedented in radiation oncology. The aim of this work is to demonstrate the feasibility of back-projection portal dosimetry for 3D dosimetric verification of Unity MR-linac treatments.

An earlier presented 2D back-projection algorithm for the Unity MR-linac geometry was extended for 3D dose reconstruction and comparison against planned dose distributions. 'In-air' as well as *in-vivo* portal EPID images can be used as input. The method was validated using data from treatments of 5 patients (2 rectal, 2 prostate cancer and one oligo metastasis). 3D pre-treatment verification of the reference plan using 'in-air' EPID images was performed and compared against planned and measured (with the Octavius 4D system) dose distributions. EPID reconstructed and planned dose distributions were compared for the first three adaptations of all treatments. For all comparisons, dose difference values at the reference point and γ-parameters (3%, 3 mm, global, in 50% isodose surface) were reported.

Pre-treatment verification against TPS data showed y_{mean} = 0.41 ± 0.04 and $y_{passrate}$ = 98.4 ± 0.1, and $\Delta Dose_{RP}$= -1.2 ± 1.3. The comparison against the OCTAVIUS 4D system showed y_{mean} = 0.37 ± 0.09 and $y_{passrate}$ = 97.4, 90% CI [95.2, 99.7], and $\Delta Dose_{RP}$= -1.4 ± 1.2. The averaged y-results for the *in-vivo* 3D verification were y_{mean} = 0.45 ± 0.09 and $y_{passrate}$ = 91.5 ± 3.1, and $\Delta Dose_{RP}$= -1.4 ± 1.2.

3D dosimetric verification of Unity MR-linac treatments using portal dosimetry is feasible, pre-treatment as well as *in-vivo*.

Keywords: MR-linac; Unity; EPID dosimetry; portal dosimetry; 3D dosimetry; QA; in-vivo

5.1. Introduction

Recently, treatment machines combining a radiation source with an MRI system have been developed and are clinically introduced. The Unity MR-linac (Elekta AB, Stockholm, Sweden) [91,92] combines a linear accelerator with a 1.5 T MRI scanner, and is equipped with an Electronic portal imaging device (EPID) mounted on the gantry, opposite to the accelerator head, allowing for simultaneous beam irradiation, EPID acquisition and MR imaging [93].

The use of EPIDs as dosimeters has been extensively studied [113,114,138,140–143,158], and their applicability for dosimetric applications has been acknowledged for pre-treatment and *in-vivo* verification of both intensity-modulated radiation therapy (IMRT) [24,58,60,144–147] and volumetric arc therapy (VMAT) [59,69,149,150].

In the Unity MR-linac, daily adaptation to patient position variations is not done by couch translations but by online replanning. In this way, patient anatomy changes can be taken into account by contour changes [94–96]. Due to the complexity of these workflows, the availability of tools for independent dosimetric verification is essential. Dosimetric verification of reference and daily adapted plans is usually performed using the combination of an MR compatible detector array and phantom. However, the use of these tools is typically time-consuming as cumbersome detector setup procedures are required. [97–100]. As a result, in most clinics dosimetric verification is limited to a few treatment fractions. Alternative patient-specific QA solutions have also been developed, such as fast sanity checks on the adapted plan [101], geometric accuracy of the delivered dose using *in-vivo* EPID images [152], or the use of independent calculations fed with linac log files [76,154,155,159,160]. These checks allow for real-time patient-specific QA that can cover most of the treatment chain, but still rely on the correct output of the machine

to generate the log files [105], and on a correct morph of the daily MRI into a synthetic CT (MRCAT) [102–104]. On the Unity system to date one of the workflows involves a density override of structures delineated on MRI scans. This presents a new element in the radiotherapy chain, which has not gone through extensive clinical validation yet, and which is not verifiable using log file based approaches.

Pre-treatment portal dosimetry using 'in-air' measurements avoids time consuming detector setup procedures as the panel is mounted on the gantry. *in-vivo* portal dosimetry provides a dosimetric end-to-end check of the online adaptation workflow making use of data acquired during treatment, i.e., without extra measurement time. Errors related to data transfer, dose delivery, patient set-up, MLC calibration, dose calculation [105], and pseudo-CT determination or density assignment can be detected. To our knowledge, portal dosimetry is the only measurement-based method for verification of pseudo-CT creating from MR data. Furthermore, portal dosimetry methods have the potential to be extended to trailing and gating techniques [89,133].

It has been shown that the dosimetric characteristics of the EPID in the Unity MR-linac are similar to conventional linacs [156,161]. Furthermore, we have shown that 2D back-projection portal dosimetry is feasible for the Unity MR-linac [162]. The aim of this study is to extend the portal dosimetry method to 3D dose reconstruction for both pre-treatment using 'in-air' measurements and in-*vivo* verification

5.2. Materials and methods

Experimental set-up

The Unity MR-linac system consists of a 7 MV flattening filter free (FFF) beam linear accelerator mounted on a ring-based gantry, built around a wide bore 1.5 T MRI scanner (Philips Medical Systems, Best,

the Netherlands). On the opposite side of the accelerator, the EPID (XRD 1642 AP, Perkin Elmer Optoelectronics, Wiesbaden, Germany) is also mounted on the ring gantry. The central region of the cryostat is designed free of gradient coils and shimming hardware, allowing for minimal and homogenous attenuation of the beam by the cryostat. The dimension of this free-of-coils region determines the size of unattenuated beams received by the EPID, allowing for a maximum field size at the isocenter of X=±11 cm and Y=±4.8 cm. Note that the EPID was included in the system for the purposes of machine QA and not for patient imaging or Portal Dosimetry, and it lies in a non-centered position with respect to the beam axis. As a result, beams can only be completely captured if their field size at isocenter is smaller than X=±11 cm, Y=[-11, +8] cm.

Images were acquired using Elekta's MVIC software. Array measurements were performed using an MR-compatible OCTAVIUS 1500 2D detector array (PTW, Freiburg, Germany), which has 1405 vented ICs with 7.1 mm center-to-center distance. For back-projection of the EPID images to the patient or phantom geometry, a research version of the IViewDose software (Elekta, AB, Stockholm, Sweden) was used.

Modifications to the model

The presented work builds on the back-projection algorithm described previously [58,70]. The first steps of adapting this method to the Unity MR-linac geometry have already been presented in previous studies [139,156,162], showing that 2D dose reconstruction in a plane through the isocenter parallel to the EPID is possible. The steps needed for implementing 3D *in-vivo* dose reconstructions are described below.

First, the algorithm was fully commissioned at gantry angle 0°, by fitting EPID data to IC measurements for different setups.

Second, the adapted gantry angle (AGA) solution for the back-projection presented in [162] was applied for the 26 gantry angle values clinically in use at the time of this study. For each gantry angle value, a sensitivity matrix was obtained by combining EPID images with 2D array measurements made at isocenter inside the OCTAVIUS rotating phantom for a 22x22 cm^2 field. Additionally, the gantry angle dependent cryostat attenuation factor was determined by fitting a back-projected 10x10 cm^2 square field at isocenter to the dose determined using the TPS.

Third, the extension from 2D to 3D dose distributions was performed similar to [58] by reconstructing the dose within the patient or phantom volume in multiple planes parallel to the EPID, obtaining the 3D dose distribution for each beam.

Fourth, the software was extended to read 3D planned dose distributions allowing for the verification of clinical plans in the patient CT, accounting for adaptations [163] in the current Unity MR-linac workflow.

Fifth, the use of virtual dose reconstruction [88] was implemented in the software allowing for 3D dose reconstruction in any geometry from 'in-air' portal images. This made pre-treatment verification possible eliminating the need using a phantom or IC array.

Finally, the parts of the beams exceeding the coil-free region of ± 4.8 cm on the cranial-caudal direction were removed, using a masking pyramid (**Figure 5.1**) per beam to both the EPID back-projected and TPS dose distributions. For all beams combined, this results in a cylinder mask in the accumulated 3D dose distribution, offering a valid comparison only in the volume where EPID images receive usable information.

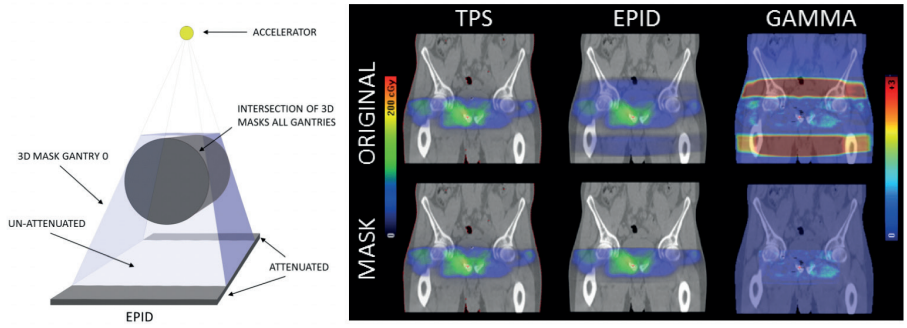

Figure 5.1: a) The EPID image is divided into the central area in which the radiation reaching the panel is minimally attenuated and the outer areas where the non-coil-free region of the cryostat causes increased attenuation. A mask is applied to the EPID reconstructed and planned dose distributions. The intersection of all masking pyramids per beam results in a cylinder per fraction. Only the un-masked volume is taken into account in the γ-evaluation. b) Planned dose, EPID reconstructed dose and γ-distributions, both without (upper row) and with the mask (lower row) applied.

Plan verification

Data from treatments of five patients were used (2 rectal-, 2 prostate cancer and one lymph node oligo metastasis patient, with 9 to 12 step-and-shoot IMRT beams). For 3D pre-treatment verification, the virtual EPID dose reconstruction of the reference plan in the OCTAVIUS phantom geometry was compared both to the array and to the TPS dose distributions calculated on the phantom geometry. The virtual EPID dose reconstruction of the reference plan was also calculated in the patient geometry and compared to the corresponding TPS patient dose distribution. For all analyses, dose difference at the reference point (ΔD_{RP}), and γ results (3%, 3 mm, 50% isodose) were reported. The isocenter was used as reference point for the OCTAVIUS phantom. The center of the PTV was used as reference point in patient dose reconstructions. For 3D *in-vivo* verification, EPID data of the first three daily adapted plans were acquired. The EPID reconstructed dose distributions were compared to their corresponding plan of the day, by

γ-analysis both in 2D per beam (3%, 3 mm, 20% isodose), and in 3D per fraction (3%, 3 mm, 50% isodose). The differences in dose value at the center of the PTV (ΔD_{PTV_C}) were also reported.

5.3. Results

Table 5.1 displays the averaged phantom pre-treatment verification results of the 5 reference plans (per site and total). Note that rectum cases present slightly worse agreement than prostate and oligo treatments.

Table 5.1: Average and standard deviation of γ-parameters (γ_{mean} , $\gamma_{passrate}$) and dose difference at reference point (ΔD_{RP}), in the comparison of virtual EPID dose distributions with both Octavius and TPS dose distributions calculated in the Octavius phantom geometry.

Site	Rectal cancer (2)	Prostate cancer (2)	Oligo metastasis (1)	Total
γ_{mean}	0.46 ± 0.04 / 0.45 ± 0.08	0.28 ± 0.03 / 0.33 ± 0.02	0.34 / 0.45	0.37 ± 0.09 / 0.40 ± 0.07
$\gamma_{passrate}$ (%)	93.7± 0.3 / 94.2 ± 3.5	99.9 ± 0.0 / 99.8 ± 0.1	99.4 / 99.2	97.4, 90% CI [95.2, 99.7] / 97.4, 90% CI [94.9, 99.9]
ΔD_{RP} (%)	-1.4 ± 0.1 / -2.8 ± 0.4	-0.7 ± 1.0 / -0.1 ± 2.1	-0.9 / 0.8	-1.4 ± 1.2 / -1.0 ± 2.0

Figure 5.2 shows pre-treatment 3D dose and γ distributions calculated in the Octavius phantom geometry for a reference prostate cancer case. Additionally, A-P and L-R profiles are also shown.

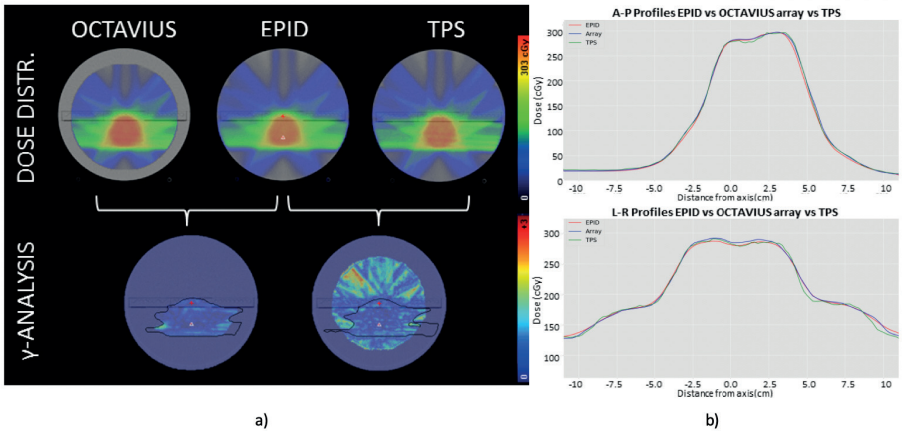

Figure 5.2: a) 3D Octavius, virtual EPID reconstructed and TPS dose distributions calculated in the Octavius phantom geometry with their corresponding γ-comparisons (3%, 2mm, global) for a prostate reference plan. The black line indicates the volume where the γ-statistics were calculated. **b**) A-P and L-R profiles through the isocenter are shown for the dose distributions.

5

Pre-treatment verification in the patient geometry using the virtual method is presented in **Figure 5.3** for a lymph node oligo metastasis treatment. In the comparison of virtual EPID with TPS dose distributions, the averaged γ-parameters of the combined results for the 5 reference plans were $\gamma_{mean} = 0.41 \pm 0.04$ and $\gamma_{passrate} = 97.9 \pm 1.7$, with an average dose difference at the center of the PTV (ΔD_{PTV}) of -0.9 % ± 0.9 %. These results compare to the agreement in phantom pre-treatment verification.

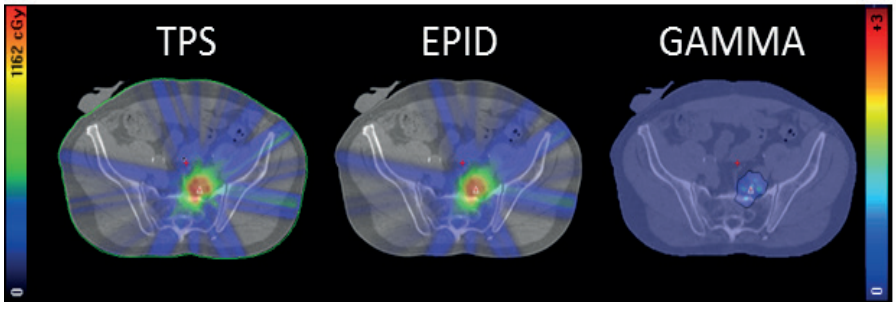

Figure 5.3: Planned and virtual EPID reconstructed dose distributions and the corresponding γ-evaluation (3%, 2mm, global) for the oligo metastasis reference plan in

the patient geometry. The color scale on the left, ranging from 0 to 1162 cGy, indicates the dose level for the TPS and EPID dose distribution maps. The color bar on the right, ranging from 0 to +3, indicates the y values for the y-map on the right figure, comparing TPS to EPID.

For the first three adapted fractions of 5 patients, **Table 5.2** presents averaged γ-parameters (γ_{mean} , $\gamma_{passrate}$) and dose difference at center of the PTV (ΔD_{PTV}) of the *in-vivo* verification for both the 3D per fraction and the 2D per beam analysis. As expected, i*n-vivo* verification shows slightly worse agreement than pre-treatment, due to extra uncertainties in the patient anatomy during the actual treatment.

Table 5.2: γ-parameters (γ_{mean} , $\gamma_{passrate}$) and dose difference at the reference point ($\%\Delta D_{RP}$) for the γ-analysis (3%, 2mm, global) in 2D per beam and in 3D per fraction, averaged over the first three fractions for the 5 patients, presented per site and total. Results are presented as average ± 1SD.

Site	**Rectum (2)**	**Prostate (2)**	**Oligo metastasis (1)**	**Total**
2D per beam Comparison EPID vs. TPS				
γ_{mean}	0.63 ± 0.14	0.56 ± 0.15	0.58 ± 0.12	0.59 ± 0.14
$\gamma_{passrate}$ (%)	80.0, 95% CI [77.7, 82.4]	84.3, 95% CI [81.7 ,87.0]	84.6, 95% CI [81.7 ,87.5]	82.7, 95% CI [81.2 ,84.3]
ΔD_{PTV} (%)	-1.4 ± 6.3	0.9 ± 6.2	3.7 ± 6.5	0.5 ± 6.6
3D per fraction Comparison EPID vs. TPS				
γ_{mean}	0.56 ± 0.04	0.48 ± 0.05	0.52 ± 0.02	0.52 ± 0.05
$\gamma_{passrate}$ (%)	88.4, 95% CI [85.2, 91.6]	95.2, 95% CI [92.1, 98.3]	95.3, 95% CI [92.9, 97.7]	92.5, 95% CI [90.2, 94.8]
ΔD_{PTV} (%)	-0.8 ± 1.2	0.9 ± 1.2	3.9 ± 1.3	0.8 ± 2.1

Note that for the oligo metastasis fractions, a somewhat large dose difference in the PTV is reported. It was observed that the center of the PTV corresponded to areas of high gradient, γ-parameters showed excellent agreement.

Figure 5.4 shows axial planes of 3D γ-distributions corresponding to the *in-vivo* verification of the first three adapted fractions of a prostate treatment.

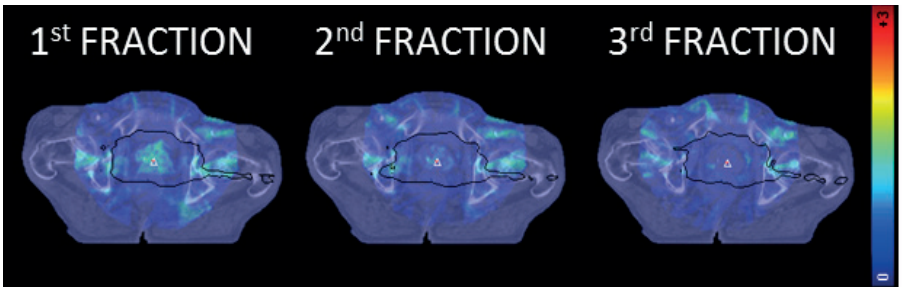

Figure 5.4: Axial planes of the 3D γ distributions (3%, 2mm, global) of the first, second and third adaptations of a prostate plan. The color scale on the right, ranging from 0 to +3 indicates the γ intensity of the 3 γ-maps.

5.4. Discussion

In this study, we have presented a method for pre-treatment and *in-vivo* 3D dosimetric verification of Unity MR-linac treatments using portal dosimetry. Treatment plans of 5 patients (3 treatment sites) were used. Comparison of the 3D back-projected EPID dose to IC array measurements using dedicated phantoms, as well as TPS dose distributions showed excellent agreement for the 5 reference plans. Moreover, the *in-vivo* results also showed good agreement when compared to the TPS for the first 3 adapted fractions. This demonstrates the feasibility of pre-treatment and *in-vivo* portal dosimetry for dosimetric verification of Unity MR-linac treatments.

The extra attenuation of the beam by the MR housing outside the window (of ±4.8 cm) in the longitudinal direction is the main limitation of the presented work, impeding the complete dosimetric verification for large target areas. However, we believe that the available (strongly attenuated) signal outside the window can be used for dosimetry purposes, although the accuracy of the final reconstructed dose distribution might be lower. Nonetheless, many of the errors that EPID dosimetry can mitigate may not necessarily require the reconstruction of the full frame as they would be alerted already in the back-projected dose distribution of the central part of the frame.

An intrinsic limitation when using the EPID for dosimetry in the MR-linac in the current setup is that parts of beams exceeding 8.1 cm in the cranial direction cannot be detected due to the non-centered position of the panel. As a result, for treatments with large fields parts of the reconstructed dose distribution will be missing, and cannot be verified. This might also lead to a possible underestimation of scatter for large fields, as parts of the beam that originate scatter are not captured by the EPID and therefore don't contribute in the determination of the primary dose.

Given the complex geometry of the MR-linac, highly density structures are affecting the EPID dose reconstruction of images in which the beam traverses the bridge or the cryostat pipe, leading to less accurate dose reconstructions for certain gantry angles. In the rectum plans of this study several of these beams were present, which in combination to the underestimation of the scatter for the large fields that was only present in the rectum treatments, resulted in worse agreement in the verification of rectum plans. To further determine whether these inaccuracies could hamper the detection of errors, more data would be required.

The presented dose reconstruction method does not account for electron return effects (ERE) caused by the presence of the magnetic field. However, as there were no large inhomogeneities present in the cases studied, we presume that in the 3D dose distributions used in this study, the ERE did not play a significant role. The performance of the method for dose verification in cases with large inhomogeneities needs further investigation. Nevertheless, for a more accurate dose reconstruction taking into account the magnetic field effects, two solutions can be considered. First is the comparison of the EPID back-projected dose distribution to a copy of the planned dose distribution calculated without the magnetic field. Alternatively, the back-projection algorithm can be used to reconstruct the fluence entering the patient and use that to feed a Monte Carlo dose engine which accounts for the magnetic field.

In conclusion, our 3D EPID dosimetry back projection algorithm was successfully adapted for the Unity MR-linac geometry, accounting for the presence of the MRI housing between patient and EPID. The presented results provide the first experimental evidence that 3D EPID dosimetry is feasible for the Elekta Unity MR-linac, both pre-treatment and in-vivo. This work presents the only independent measurement-based QA solution of the entire online adaptive chain including the use of a pseudo-CT and paves the way for the development of an automated verification solution for the online adaptive workflow of the Elekta Unity MR-linac.

5.5. Disclosure of conflicts of interest

Support for this research was provided, in part, by Elekta AB, Stockholm, Sweden.